Waveguide-Plasmon Polaritons: Strong Coupling of Photonic and Electronic Resonances in a Metallic Photonic Crystal Slab

A. Christ,[1] S. G. Tikhodeev,[2,1] N. A. Gippius,[2,3] J. Kuhl,[1] and H. Giessen[4]
[1]*Max-Planck-Institut für Festkörperforschung, 70569 Stuttgart, Germany*
[2]*General Physics Institute RAS, Vavilova 38, Moscow 119991, Russia*
[3]*Institute of Physical and Chemical Research (RIKEN), Wako 351-0198, Japan*
[4]*Institute of Applied Physics, University of Bonn, 53115 Bonn, Germany*
(Received 20 December 2002; published 28 October 2003)

Strong coupling between localized particle plasmons and optical waveguide modes leads to drastic modifications of the transmission of metallic nanowire arrays on dielectric waveguide substrates. The coupling results in the formation of a new quasiparticle, a waveguide-plasmon polariton, with a surprisingly large Rabi splitting of 250 meV. Our experimental results agree well with scattering-matrix calculations and a polariton-type model. The effect provides an efficient tool for photonic band gap engineering in metallodielectric photonic crystal slabs. We show evidence of a full one-dimensional photonic band gap in resonant plasmon-waveguide structures.

DOI: 10.1103/PhysRevLett.91.183901 PACS numbers: 42.70.Qs, 73.20.Mf, 78.66.–w

The optical properties of materials can be efficiently manipulated by periodic structuring on a scale comparable to the wavelength of light [1]. Similarly to the commonly employed dielectric structures, photonic crystals based on metals provide remarkable optical properties, which includes focusing of light into small volumes and the enhancement of light transmission through subwavelength hole arrays [2]. Collective electronic excitations called particle or surface plasmons are the main physical mechanism behind these effects (see, e.g., [3], and references therein).

Waveguiding metallic photonic crystals belong to the new material class of so-called active photonic crystals. They provide *simultaneous* electronic and photonic resonances in the same energy range. Both resonances can be influenced by geometrical structuring of the sample on a nanometer scale. Thus their interaction can be controlled and, in the case of strong coupling, the formation of a new quasiparticle can be expected. Other types of active photonic crystals have been investigated previously, using an exciton-waveguide resonance [4,5], but we will demonstrate that the plasmon-waveguide interaction in metallic photonic crystals can be much stronger.

In this Letter, we investigate one-dimensional (1D) periodic gold nanowire arrays on top of a dielectric waveguide as an ideally suited model system. Comparing our work with previous investigations on metal gratings (see, e.g., [6]), we would like to emphasize the importance of the waveguiding layer in our system. We observe strong interaction of the localized wire plasmons with the quasiguided photon modes in this photonic crystal structure. The result is the formation of a waveguide-plasmon polariton with a large Rabi splitting of about 250 meV. The waveguide-plasmon resonance provides a novel and efficient tool for photonic band gap (PBG) engineering in metallic photonic crystal slabs (PCS). For example, a full overlap of the stop bands for all polarizations (a full 1D PBG) can occur for guided light propagating normal to the wires in the case of resonance between photons and nanowire plasmons. In contrast to nanodots [7,8], localized plasmons in nanowires are excited only by incoming light that is polarized perpendicular to the nanowires (TM polarization). The modifications of the optical properties in our model system are spectacular due to the large optical strength of the nanowire plasmons. In this Letter, we show excellent agreement between our experimental results and model calculations, supporting our polariton picture.

We used electron beam lithography to prepare 1D gold gratings on top of 140-nm-thick indium tin oxide (ITO) waveguide layers deposited on a quartz substrate. For the produced sample series, the grating period d_x was increased from 375 to 575 nm in steps of 25 nm, while the grating height of 20 nm and the wire width of 100 nm were kept fixed. The grating extension was restricted to $100 \times 100\ \mu\text{m}^2$. The aperture angle of the transmitted white light beam was reduced below 0.2° [8]. Figure 1 shows the experimental geometry [panels (a),(b)] and the measured extinction spectra [panel (c)]. The latter are drastically different from those measured in the structure with a thin ITO layer [panel (d)], which does not support guided modes.

For the theoretical calculations, we employed the scattering-matrix method [9,10], decomposing the electromagnetic field into planar waves with momenta $k_{g,x} = k_x + K_g$, $K_g = 2\pi g/d_x$, $g = 0, \pm 1, \pm 2, \ldots, \pm G$, where $k_x = \omega \sin\vartheta/c$, ω and ϑ are the incoming photon frequency and angle of incidence (see Fig. 1) [11]. The measured (top panels in Fig. 2) extinction spectra for varying periods and angles of incidence are in very good qualitative agreement with the calculated ones (bottom panels). The only parameters in the calculations are the geometric sizes and the dielectric constants of quartz (2.13), ITO [13], and gold [14]. We emphasize

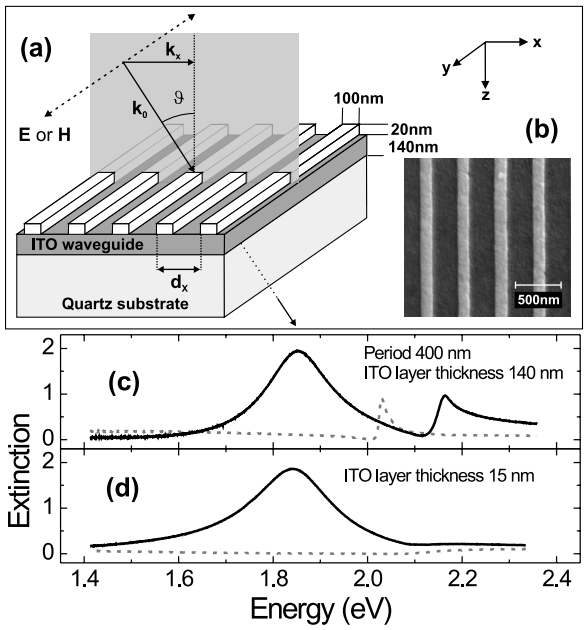

FIG. 1. Schematic view (a), electron micrograph (b), and measured extinction [$-\ln(T)$, T: transmission] spectra (c) of the gold wire array on top of a 140-nm-thick ITO waveguide; (d) same as (c) with a 15-nm-thick ITO layer. The dashed arrows in (a) show the electric (magnetic) field direction for TE (TM) polarization. $\mathbf{k}_0$ is the incident light wave vector. The extinction spectra are represented by solid lines and dashed lines for TM and TE polarization, respectively.

here that there is *no adjustable parameter* in these calculations.

The measured as well as calculated extinction spectra show pronounced peaks with a complex behavior versus period and/or angle. The energy positions of the maxima in the measured and calculated spectra are shown in Fig. 3 (top panels) as solid and open symbols, respectively. Our calculations show that the electromagnetic field near the gold wires is increased resonantly at photon energies near the extinction maxima. Thus, the maxima rather than the minima correspond to the resonant modes (as had been suggested incorrectly in [7]).

Let us first discuss TE polarization [dashed lines in Figs. 1(c) and 2(a) and stars in Fig. 3(a)]. The narrow peaks in the TE spectra are due to excitation of TE quasiguided modes; they do not appear in structures with a thin ITO layer that does not support guided modes [Fig. 1(d)]. Such resonant modes are the characteristic feature of waveguiding PCS (see, e.g., [10,15], and references therein). In our case they arise due to the Bragg resonance of TE_0 waveguide modes with $K_\pm = \pm 2\pi/d_x$ in the ITO layer. They are examples of Fano-type resonances due to the interaction of the discrete waveguide mode with the photon continuum. Only the upper symmetric quasiguided mode is seen at normal incidence, as common for structures with mirror symmetry, whereas the lower mode becomes antisymmetric and optically inactive [5]. The energy interval between the upper and lower modes is the 1D PBG for TE light propagating inside the waveguide along the $\hat{\mathbf{x}}$ direction.

In TM polarization [solid lines in Fig. 1(c) and 2 and circles in Fig. 3], a broader peak appears around 1.9 eV, in addition to the narrow peaks due to TM_0 quasiguided modes [the latter are absent in structures with a thin ITO layer; see Fig. 1(d)]. This broader peak is due to a particle plasmon in an individual gold wire. With the change of the period and/or angle, this broad plasmon line shows an anticrossing behavior with the narrower TM-waveguide resonances. Two peaks can be seen in TM polarization at normal incidence [Figs. 1(c) and 2(a)], and a third peak appears between them *only* at inclined incidence [Figs. 2(b) and 2(c)] [8]. As in the TE case, the absence of the third peak for normal incidence in TM is a consequence of the mirror symmetry of the structures.

The anticrossing behavior can be easily explained in terms of the formation of a new quasiparticle: polariton-type coupled modes emerge from the "bare" modes near the center of the first Brillouin zone (BZ). The bare modes are the gold wire plasmons and the lowest TM_0 waveguide photons with momenta around $K_\pm$. The effective Hamiltonian near the center of the first BZ can be written as

$$H_{\text{eff}} = \begin{pmatrix} E(K_+ + k_x) & V_1 & V_2 \\ V_1 & E(K_- + k_x) & V_2 \\ V_2 & V_2 & E_{\text{pl}} \end{pmatrix}, \quad (1)$$

where $E(k)$ are the bare energies of TM_0 guided modes with momenta $K_\pm + k_x$, E_{pl} is the individual wire plasmon energy, V_1 is the PBG half-width in the 1D PCS, and V_2 is the waveguide photon-wire plasmon coupling energy. Because of the mirror symmetry of the structure, $E(K_\pm + k_x) \approx E_0 \pm \tilde{c}k_x$, where E_0 and $\tilde{c}$ are the TM_0 mode energy and the group velocity, respectively, near momenta $\approx K_\pm$.

Because of the absorption of light in the metal, all modes have finite linewidths. This can be accounted for using a non-Hermitian effective energy matrix instead of Eq. (1), substituting in Eq. (1) E and E_{pl} by $E - i\gamma$ and $E_{\text{pl}} - i\Gamma$, where γ and Γ are the half-widths of the waveguide modes and wire plasmon. The radiative losses of quasiguided modes [10] have to be included too. This can be accomplished assuming that the photonic band gap in the PCS is complex, replacing V_1 by $V_1 - i\gamma_1$, where γ_1 is the radiative damping of the quasiguided modes. Symmetrizing and antisymmetrizing the first two rows in Eq. (1), we get the effective energy matrix

$$\begin{pmatrix} E_0 + V_1 - i(\gamma + \gamma_1) & \tilde{c}k_x & \sqrt{2}V_2 \\ \tilde{c}k_x & E_0 - V_1 - i(\gamma - \gamma_1) & 0 \\ \sqrt{2}V_2 & 0 & E_{\text{pl}} - i\Gamma \end{pmatrix}, \quad (2)$$

where the first (second) row represents the energy of the symmetrized (antisymmetrized) photonic mode. It can be seen that the antisymmetrized mode is decoupled from

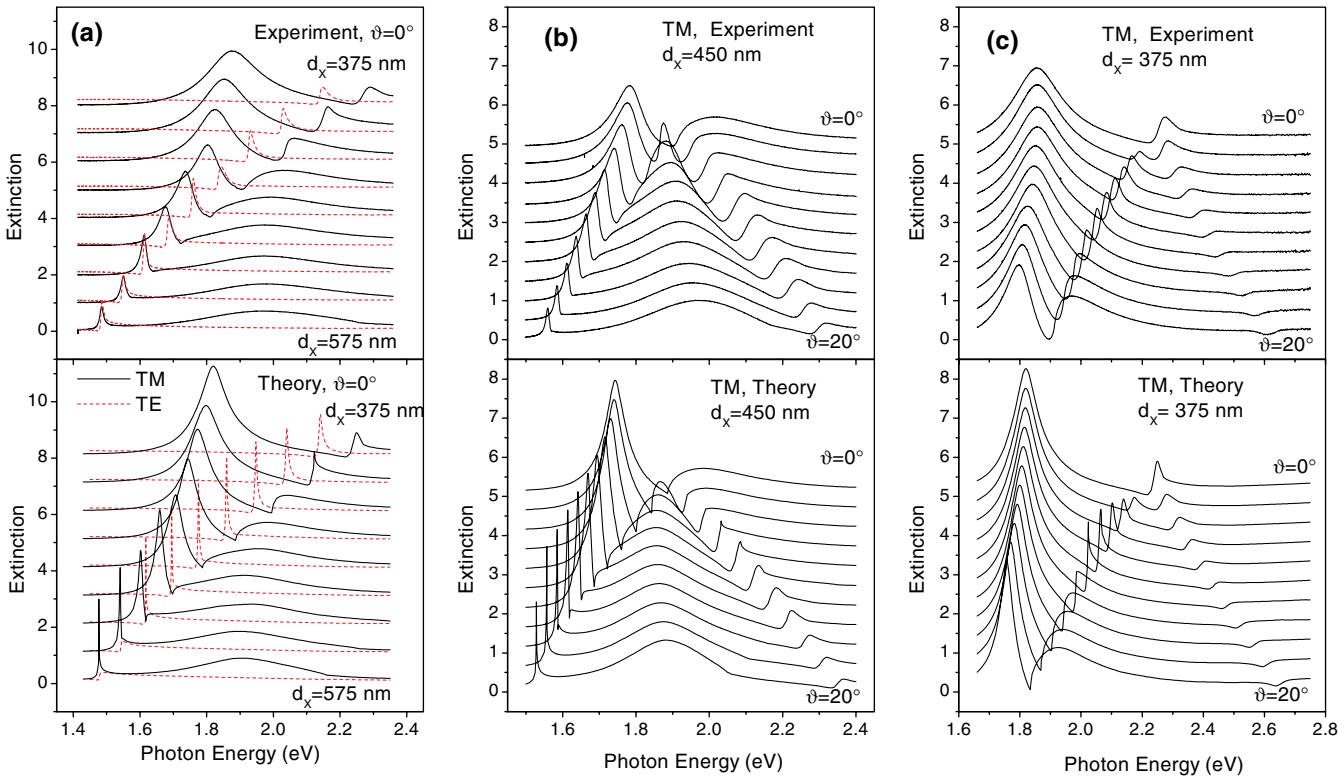

FIG. 2 (color online). Measured (top panels) and calculated (bottom panels) extinction spectra: (a) normal light incidence and nanowire arrays with periods from 375 to 575 nm; (b),(c) light incidence with angle ϑ from 0° to 20° in nanowire arrays with periods of 450 and 375 nm, respectively.

the plasmon and from the symmetrized mode at $k_x = 0$, i.e., in the center of the first BZ. At $k_x \neq 0$ this mode is coupled with the plasmon only indirectly, via the coupling to the symmetrized mode.

The behavior of the eigenenergies of the matrix equation in (2) reproduces the behavior of the maxima in the extinction spectra and of the linewidths surprisingly well, as demonstrated by the lines in Fig. 3. To draw these lines,

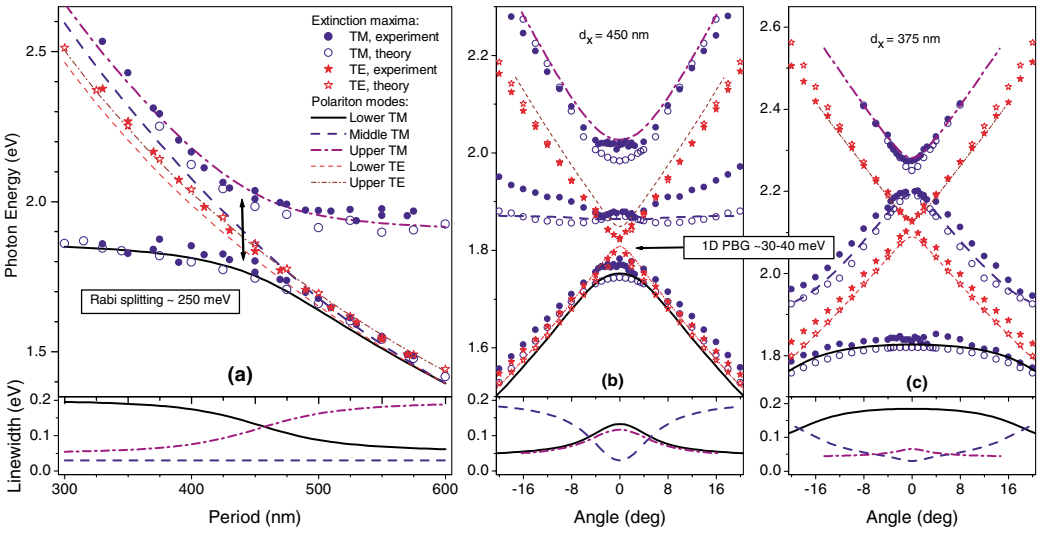

FIG. 3 (color online). Measured and calculated positions of the extinction spectra maxima (solid symbols and open symbols in top panels) in TE (stars) and TM (circles) polarization. The dependences vs d_x and ϑ are given in (a) and (b),(c), respectively. Thick lines are the dispersions of the three TM waveguide-plasmon polariton modes near the center of the first BZ: real and imaginary parts of the eigenenergies of Eq. (2) are shown in the top and bottom panels, respectively. The thin lines are the corresponding two TE quasiguided modes (shown only in the top panels). The arrows show the polariton Rabi splitting and the full 1D PBG.

we have used the calculated dispersion of TE_0 and TM_0 waveguide modes in a 140-nm-thick ITO waveguide on quartz and the fitted values: $E_{\mathrm{pl}}, \Gamma, \gamma, \gamma_1, V_1, V_2 =$ 1875, 100, 20, 5, 20, 100 meV. The PBG half-width V_1 was taken from the results for the PBG from the exact scattering-matrix calculations. Presumably, these parameters (including their dependences on photon energy and horizontal components of the momentum) can be rigorously calculated within a resonance approximation to the scattering matrix. Here, however, we treat them as reasonably adjustable parameters.

According to the measurements and exact calculations, the Rabi splitting between the lower and upper polariton branches at $\vartheta = 0$ is ≈ 250 meV. In the polariton model, this is equal to $\sqrt{8V_2^2 - (\Gamma - \gamma - \gamma_1)^2}$. It allows one to fit the value of V_2, using also the measured plasmon mode linewidth far from the resonance. Because $\Gamma \gg \gamma, \gamma_1$, the modes in Fig. 3 depend on γ and γ_1 only weakly.

A whole set of interesting features of the waveguide-plasmon resonance versus period and angle are qualitatively reproduced well in the polariton model (see Fig. 3). Actually, in the real system the shape of the peaks in extinction is highly nonsymmetric due to the Fano-type nature of these resonances [10]. In this case, the positions of the maxima in extinction do not necessarily coincide with the mode eigenenergies. In real systems the PBG width and other parameters are energy dependent. Thus, only a qualitative agreement of the polariton model with the real extinction spectra is possible.

Note that a full 1D photonic band gap, i.e., full overlap of stop bands for light propagating in the waveguide along $\hat{\mathbf{x}}$ having *any* polarization, occurs near the wire plasmon resonance [see Fig. 3(b), for $d_x = 450$ nm]. This feature is a promising property of metal-based PCS which may be of importance for possibly creating defect waveguides and microresonators based on such PCS.

In addition, we would like to mention a difference of the waveguide-plasmon polariton state in metal-based PCS analyzed here from the exciton-polariton in PCS containing a semiconductor [5]. In the waveguide-plasmon polariton case, a full anticrosssing of both polariton branches is observable, while in the semiconductor case the excitonic extinction peak remains always visible.

In conclusion, we have shown experimentally and theoretically that strong coupling between electronic and photonic resonances in metallic photonic crystals leads to the formation of new quasiparticles. In particular, we demonstrate that coupling the particle plasmon resonances in gold nanowire arrays to optical waveguide modes results in the formation of a waveguide-plasmon polariton with a large Rabi splitting of 250 meV. This novel effect is a suitable tool for photonic band gap engineering in active photonic crystals.

This work was financially supported by the German Bundesminister für Bildung und Forschung (FKZ 13N8340/1), the Deutsche Forschungsgemeinschaft (Priority Program SP1113), and in part by the Russian Foundation for Basic Research and the Russian Ministry of Science. The authors are grateful to K. von Klitzing for continuous support and to T. Ishihara, S. Linden, E. A. Muljarov, V.V. Popov, and F. J. Garcia-Vidal for discussions.

[1] E. Yablonovitch, Phys. Rev. Lett. **58**, 2059 (1987); S. John, Phys. Rev. Lett. **58**, 2486 (1987); J. D. Joannopoulos, R. D. Meade, and J. N. Winn, *Photonic Crystals* (Princeton University, Princeton, NJ, 1995); C. Weisbuch *et al.*, Phys. Rev. Lett. **69**, 3314 (1992).

[2] J. Pendry, Science **285**, 1687 (1999); H. J. Lezec *et al.*, Science **297**, 820 (2002).

[3] U. Kreibig and M. Vollmer, *Optical Properties of Metal Clusters* (Springer, Berlin, 1995).

[4] L. Pilozzi, A. D'Andrea, and R. D. Sole, Phys. Rev. B **54**, 10 763 (1996).

[5] A. L. Yablonskii *et al.*, J. Phys. Soc. Jpn. **70**, 1137 (2001).

[6] R. H. Ritchie *et al.*, Phys. Rev. Lett. **21**, 1530 (1968); G. Schider *et al.*, J. Appl. Phys. **90**, 3825 (2001).

[7] S. Linden, J. Kuhl, and H. Giessen, Phys. Rev. Lett. **86**, 4688 (2001).

[8] It is important to notice that the experiments in Ref. [7] were performed with focused light with an aperture of $\approx 3°$. Therefore the spectra revealed a distinct middle peak at normal incidence, due to the limited angular resolution of the setup. Recent repetition of the experiment on 2D structures with high angular resolution proved that this peak disappears at normal incidence for nanodot arrays as well [S. Linden, Ph.D. thesis, Marburg, 2001].

[9] D. M. Whittaker and I. S. Culshaw, Phys. Rev. B **60**, 2610 (1999).

[10] S. G. Tikhodeev *et al.*, Phys. Rev. B **66**, 045102 (2002).

[11] Although in the limit $G \to \infty$ this decomposition is asymptotically exact, we truncate the matrices at $N_G = 2G + 1$ in the numerical calculations. The TE spectra in Fig. 2 were calculated with $N_G = 49$ with a relative error smaller than 0.01%. The convergence in TM is slower, although we employed the idea of Ref. [12], significantly improving the convergence. The TM spectra were calculated with $N_G = 301$, with an estimated relative error $\approx 1\%$. The slow convergence makes the Fourier-series based theory for 2D metal arrays impractical because as much as 300×300 harmonics are needed.

[12] P. Lalanne and G. M. Morris, J. Opt. Soc. Am. A **13**, 779 (1996).

[13] Experimental values of the ITO dielectric constant [R. Parmentier *et al.* (private communication)] were fitted by $\varepsilon_{\mathrm{ITO}}(\lambda) \approx 1 + 1.813\,02\lambda^2/(\lambda^2 - 0.075\,97)$ for λ between 0.3 and 0.6 μm.

[14] P. B. Johnson and R.W. Christy, Phys. Rev. B **6**, 4370 (1972).

[15] S. Fan and J. D. Joannopoulos, Phys. Rev. B **65**, 235112 (2002).